IBRO Neuroscience Reports 11 (2021) 73–80

Contents lists available at ScienceDirect

IBRO Neuroscience Reports

journal homepage: www.sciencedirect.com/journal/IBRO-Neuroscience-Reports

Research Paper

Mid-pregnancy maternal immune activation increases Pax6-positive and Tbr2-positive neural progenitor cells and causes integrated stress response in the fetal brain in a mouse model of maternal viral infection

Tsuyoshi Tsukada [a,b,*], Hiromi Sakata-Haga [a], Hiroki Shimada [c], Hiroki Shoji [d], Toshihisa Hatta [a,*]

[a] Department of Anatomy, Kanazawa Medical University, Uchinada, Ishikawa 920-0293, Japan
[b] Department of Neurosurgery, Kanazawa Medical University, Uchinada, Ishikawa 920-0293, Japan
[c] Department of Medical Science, Kanazawa Medical University, Uchinada, Ishikawa 920-0293, Japan
[d] Department of Biology, Kanazawa Medical University, Uchinada, Ishikawa 920-0293, Japan

ARTICLE INFO

Keywords:
Maternal immune activation
Polyriboinosinic–polyribocytidylic acid
Integrated stress response
Activating transcription factor 4
Unfolded protein response
Neurogenesis

ABSTRACT

Maternal immune activation (MIA) in midpregnancy is a risk factor for neurodevelopmental disorders. Improper brain development may cause malformations of the brain; maldevelopment induced by MIA may lead to a pathology-related phenotype. In this study, a single intraperitoneal injection of 20 mg/kg polyriboinosinic–polyribocytidylic acid [poly(I:C)] was administered to C57BL/6J mice on embryonic day (E) 12.5 to mimic maternal viral infection. Histopathological analysis of neurogenesis was performed using markers for Pax6, Tbr2, and Tbr1. In these fetuses, significant increases were observed in the proportion of Pax6-positive neural progenitor cells and Pax6/Tbr2 double-positive cells 24 h after poly(I:C) injection. There were no differences in the proportion of Tbr1-positive postmitotic neurons 48 h after poly(I:C) injection. At E18.5, there were more Pax6-positive and Tbr2-positive neural progenitor cells in the poly(I:C)-injected group than in the saline-injected group. Gene ontology enrichment analysis of poly(I:C)-induced differentially expressed genes in the fetal brain at E12.5 demonstrated that these genes were enriched in terms including response to cytokine, response to decreased oxygen levels in the category of biological process. At E13.5, activating transcription factor 4 (Atf4), which is an effector of integrated stress response, was significantly upregulated in the fetal brain. Our results show that poly(I:C)-induced MIA at E12.5 leads to dysregulated neurogenesis and upregulates Atf4 in the fetal brain. These findings provide a new insight in the mechanism of MIA causing improper brain development and subsequent neurodevelopmental disorders.

Introduction

Epidemiological studies have suggested that maternal infection in midpregnancy is a risk factor for neurodevelopmental disorders in the offsprings (Atladóttir et al., 2009; Brown, 2006; Brown et al., 2004, 2001). A model of neurodevelopmental disorders induced by maternal immune activation (MIA) has aided in understanding the mechanisms behind these developments (Carpentier et al., 2011, 2013; Choi et al., 2016; Hsiao and Patterson, 2011; Shi et al., 2005; Smith et al., 2007; Stolp et al., 2011; Tsukada et al., 2018, 2015; Wu et al., 2017). The basis for development of autism spectrum disorders (ASD), one of the neurodevelopmental disorders, has been shown to involve improper developmental processes such as neurogenesis, neurite growth, synaptogenesis, and synaptic plasticity (Gilbert and Man, 2017). Improper developmental processes have well-known causes and underlying mechanisms for the development of malformations of the brain; pathological studies of ASD brains have shown changes in the number of neurons in early childhood (Courchesne et al., 2011), defects of

Abbreviations: MIA, Maternal immune activation; ASD, autism spectrum disorders; [polyI:C], polyriboinosinic–polyribocytidylic acid; DEG, differentially expressed gene; ISR, integrated stress response; Atf4, activating transcription factor 4; UPR, unfolded protein response; NPCs, neural progenitor cells; SVZ, subventricular zone; VZ, ventricular zone; CP, cortical plate.

* Corresponding author at: Department of Anatomy, Kanazawa Medical University, Uchinada, Ishikawa 920-0293, Japan.
* Corresponding author.
E-mail addresses: ttsukada@kanazawa-med.ac.jp (T. Tsukada), thatta@kanazawa-med.ac.jp (T. Hatta).

https://doi.org/10.1016/j.ibneur.2021.07.003
Received 8 March 2021; Accepted 31 July 2021
Available online 3 August 2021

neurogenesis and neuronal migration, and dysplastic changes (Stoner et al., 2014; Wegiel et al., 2010). In this context, it is reasonable to expect that impairment in any of these processes could cause abnormal brain development leading to neurodevelopmental disorders. In fact, neuroimaging MRI studies have shown that malformations in cortical development disrupted structural and functional brain networks (Hong et al., 2017). In line with this notion, a recent study elucidated the role of IL-17 in the pathophysiological mechanism of cortical dyslamination of somatosensory areas, leading to an ASD phenotype in a model of neurodevelopmental disorders induced by MIA (Shin Yim et al., 2017). In addition, the size of some cortices, including the somatosensory cortex, decreased in offsprings exposed to MIA (Kreitz et al., 2020). Aside from these findings, we have demonstrated that MIA decreases proliferation of neural progenitor cells (NPCs) at midgestation and decreases cell numbers in the dorsolateral cortex at late gestation (Tsukada et al., 2015). These data suggest that impaired neurogenesis is a key causative mechanism for the development of malformations of the brain. However, the underlying mechanisms leading to impaired neurogenesis, which could be integrated and translated into clinical settings, have not yet been elucidated. As an individual mechanism of impaired neurogenesis after MIA, it has been shown that hypoxia (Carpentier et al., 2013) and cytokine attack (Gallagher et al., 2013) caused deregulation of NPCs. Recently, it has been suggested that the unfolded protein response (UPR) regulates neurogenesis in the fetal brain by affecting the balance between direct neurogenesis and indirect neurogenesis, that is, by reducing intermediate progenitors that generate cortical neurons (Canetta et al., 2016; Godin et al., 2016; Laguesse et al., 2015). Furthermore, direct prenatal Zika virus infection can cause microcephaly by activating transcription factor 4 (Atf4)-mediated UPR, which affects neurogenesis (Alfano et al., 2019; Gladwyn-Ng et al., 2018). We hypothesized that MIA causes impairment of neurogenesis in relation to UPR. It is well known that direct neurogenesis occurs via Pax6-positive NPCs and indirect neurogenesis via Tbr2-positive NPCs (Arai et al., 2011; Götz and Huttner, 2005). These two transcription factors are sequentially expressed by different classes of neurogenic NPCs, and another transcription factor, Tbr1, is expressed by postmitotic neurons in the developing cortex (Englund et al., 2005). Since there are no detailed histopathological analyses of neurogenesis using markers for Pax6, Tbr2, and Tbr1 in MIA, we first performed immunohistochemical analysis to confirm impaired neurogenesis. Next, we examined whether MIA could cause integrated stress response (ISR) leading to UPR in the fetal brain with bioinformatics analysis, quantitative real-time PCR.

Materials and methods

Animals

Male and female C57BL/6J mice (Japan SLC, Inc., Hamamatsu, Japan) were used in this study. The mice were maintained under standard laboratory conditions. Food and water were available ad libitum. A female mouse was housed with a male mouse overnight, and the day on which a vaginal plug was found in the morning was designated as embryonic day (E) 0.5. All procedures in this study were performed in strict accordance with the guidelines for the Care and Use of Laboratory Animals of Kanazawa Medical University, Ishikawa, Japan. The protocol was approved by the Committee on the Ethics of Animal Experiments of Kanazawa Medical University (Protocol number 2017-51). Procedures were performed using the anesthetic combination of midazolam (4 mg/kg), medetomidine (0.3 mg/kg), and butorphanol (5 mg/kg), and all efforts were made to minimize suffering.

MIA treatment

At E12.5, pregnant females were administered an intraperitoneal injection of poly(I:C) (Sigma-Aldrich, St. Louis, MO, USA) at 20 mg poly (I:C)/kg mouse weight (Smith et al., 2007). The injection volume was adjusted to 10 μl/g body weight. Control mice were injected with an equivalent volume of saline. Pregnant mice were sacrificed at E13.5 (24 h after the injection), E14.5 (48 h after the injection), or E18.5 under deep anesthesia, and fetuses were quickly collected for subsequent histochemical and molecular biological analyses.

Quantitative real-time polymerase chain reaction (PCR)

For the extraction of total RNA from paraffin-embedded fetal brain sections (15 μm thick) at E13.5, we used the ISOGEN PB kit (Nippon Gene Co., LTD., Tokyo, Japan). The quality and concentration of extracted RNA were assessed using a DS-11 NanoPad (DeNovix, Wilmington, DE, USA). Genomic DNA was digested using DNase-I following the manufacturer's instructions (Nippon Gene Co., LTD.). Reverse transcription was performed with DNase-I–treated RNA as a template using SuperScript VILO reverse transcriptase (Thermo Fisher Scientific). Quantitative PCR was conducted with GeneAce SYBR® qPCR Mix α (Nippon Gene Co., LTD.); 18S ribosomal RNA was used as an internal control. The expression levels of activating transcription factor 4 (*Atf4)* were determined; 18S ribosomal RNA forward and reverse primers were used: 5′-AGGAATCAAAATTTAAGGAAA-3′ and 5′-TTTGTCTGTCGGAAGATATG-3′. Atf4 forward and reverse: 5′-CCTAGGTCTCTTAGATGACTATCTGGAGG-3′ and 5′-CCAGGTCATCCATTCGAAACAGAGCATCG-3′. PCR reactions were conducted in duplicate using the Thermal Cycler Dice® Real Time System (TaKaRa Bio Inc, Kusatsu, Japan) and quantified using the delta–delta-cycle threshold (Ct) method ($2^{-\Delta\Delta Ct}$) (Livak and Schmittgen, 2001). Dissociation curve analysis was used to confirm the specificity of the PCR products.

Immunohistochemistry

Coronal sections of paraffin-embedded fetal brains were obtained (15 μm thick) and adhered to glass slides. Immunohistochemical analyses using 3,3′-diaminobenzidine (DAB) staining were conducted on these tissues. The sections were microwaved in 10 mM citrate buffer (pH 6.0) for Pax6 and Tbr2 staining or 10 mM TE buffer (pH 9.0) for Atf4 staining. Endogenous peroxidase activity was quenched with 3% hydrogen peroxide in methanol for 10 min. The sections were blocked with 1% bovine serum albumin in phosphate-buffered saline containing 0.1% Triton X-100 (PBST). After washing with PBST, the sections were incubated with the primary antibodies at 4 °C overnight. Primary antibodies included rabbit anti-Pax6 pAb (1:2000; FUJIFILM Wako Pure Chemical Corporation, Osaka, Japan) and anti-Tbr2 pAb (1:2500; Abcam plc, Cambridge, UK). Nonimmune rabbit IgG (Sigma-Aldrich Co. LLC, MO, USA) was used as the negative control. After washing with PBST, the sections were incubated with Envision+ System-HRP Labelled Polymer Anti-Rabbit following the manufacturer's instructions (Agilent Technologies, CA, USA), visualized using DAB substrate (Agilent Technologies), and counterstained with hematoxylin before dehydration. The sections were subsequently coverslipped and imaged using a NanoZoomer C9600–03 (Hamamatsu Photonics K.K., Hamamatsu, Japan). For immunofluorescence staining, specific staining of Pax6, Tbr2, and Tbr1 was conducted using the Opal™ 4-Color Manual IHC Kit (PerkinElmer Japan Co., Ltd., Yokohama, Japan) following the manufacturer's instructions. For staining of Tbr1, we used anti-Tbr1 pAb (1:2000; Abcam) and secondary antibodies identical to those mentioned previously. As a negative control, we used nonimmune mouse IgG (Sigma-Aldrich). Images were visualized using an LSM 710 confocal microscope (ZEISS, Oberkochen, Germany). The sections were chosen from the dorsolateral regions located anterior to the primitive hippocampus since previous studies have reported that MIA at midgestation decreases the cortical area of the prefrontal association cortex in offsprings (Kreitz et al., 2020) and induces more disorganization of cortical wall lesions in the anterior part of the brain (Shin et al., 2017).

Quantitative analysis of histological findings

We used QuPath software (v0.2.0) (Bankhead et al., 2017) to

evaluate immunohistochemical data. Cells were counted in fluorescent images obtained with 40 × oil immersion magnification. A total of 4–6 sites on three slices for every 10th section were analyzed for each brain. For this analysis, multiple brain slices from three fetuses at E13.5, four fetuses at E14.5, and two fetuses at E18.5 were quantified per group. Quantitative analysis was performed within the columnar areas of 100 μm width for E13.5 and E14.5, from ventricular zone (VZ) to cortical plate (CP). For slices at E18.5, we performed the analysis within the columnar area of 50 μm of the brain wall.

Bioinformatics analysis of microarray data

Processed gene expression microarray data was obtained from the article published in Translational Psychiatry (Garbett et al., 2012). The data has been published as Supplemental Material 2 in the article. Briefly, pregnant mice at E12.5 were injected with saline, or poly(I:C) intraperitoneally at 20 mg poly(I:C)/kg mouse weight. Then, pregnant mice were euthanized 3 h after poly(I:C) injection. Extracted RNA quality from fetal brains was assessed using an Agilent (Palo Alto, CA, USA) Bioanalyzer. Differentially expressed genes were noted as based on the following points: (1) average log 2 ratio > 30%, and (2) $P < 0.05$ using the Student's *t*-test. We extracted genes that corresponded to candidate DEGs in the fetal brain exposed to maternal injection with poly (I:C) following these steps. First, three different methods were employed to induce MIA. DEGs were divided into three groups. First, from the "A. Changed in all 3 MIA models" list, all genes were extracted. Second, from the "B. Changed in 2 of 3 MIA models" list, genes relevant to the poly (I:C)-injected group were extracted. Third, from the "C. Changed in 1 of 3 MIA models" list, genes relevant to the poly (I:C)-injected group were extracted. By combining these three gene lists and converting them into Entrez ID, we extracted gene identities and transferred them into a GO enrichment analysis tool. A total of 228 of DEGs were analyzed by functional enrichment analyses to detect which gene ontology (GO) terms are significantly over-represented using ShinyGO v0.61 (Ge et al., 2020).

Statistical analyses

Data are presented as means ± standard error. All statistical analyses were performed using R 4.0.0 (https://www.r-project.org). Two-way ANOVA and unpaired two-tailed Student's *t*-tests were employed. *P*-values of < 0.05 were considered significant for all experiments in this study.

Results

MIA acutely increased the proportion of Pax6-positive cells

To examine the composition of NPCs after MIA at E12.5, we first performed immunohistochemical analysis with two progenitor markers, Pax6 and Tbr2, at E13.5 after 24 h from maternal poly(I:C) injection. In the saline-injected and poly(I:C)-injected groups, as in normal development, Pax6-positive cells and Tbr2-positive cells were mainly located in the VZ and the subventricular zone (SVZ), respectively (Fig. 1A–F). Quantitative analysis revealed there were significantly increased proportions of Pax6-positive cells in the poly(I:C)-injected group (Fig. 1G). Conversely, the proportion of Tbr2-positive cells was not significantly different between both groups (Fig. 1G). However, the proportion of Pax6/Tbr2 double-positive cells was also significantly increased in the poly(I:C)-injected group compared to that in the saline-injected group (Fig. 1G). In the developing neocortex, Tbr2-positive basal progenitor cells (BPs) are generated from Pax6 positive radial glia, and only produce neurons. In this postmitotic neuron production, neural progenitor cells upregulate Tbr2 and downregulate Pax6 along with the

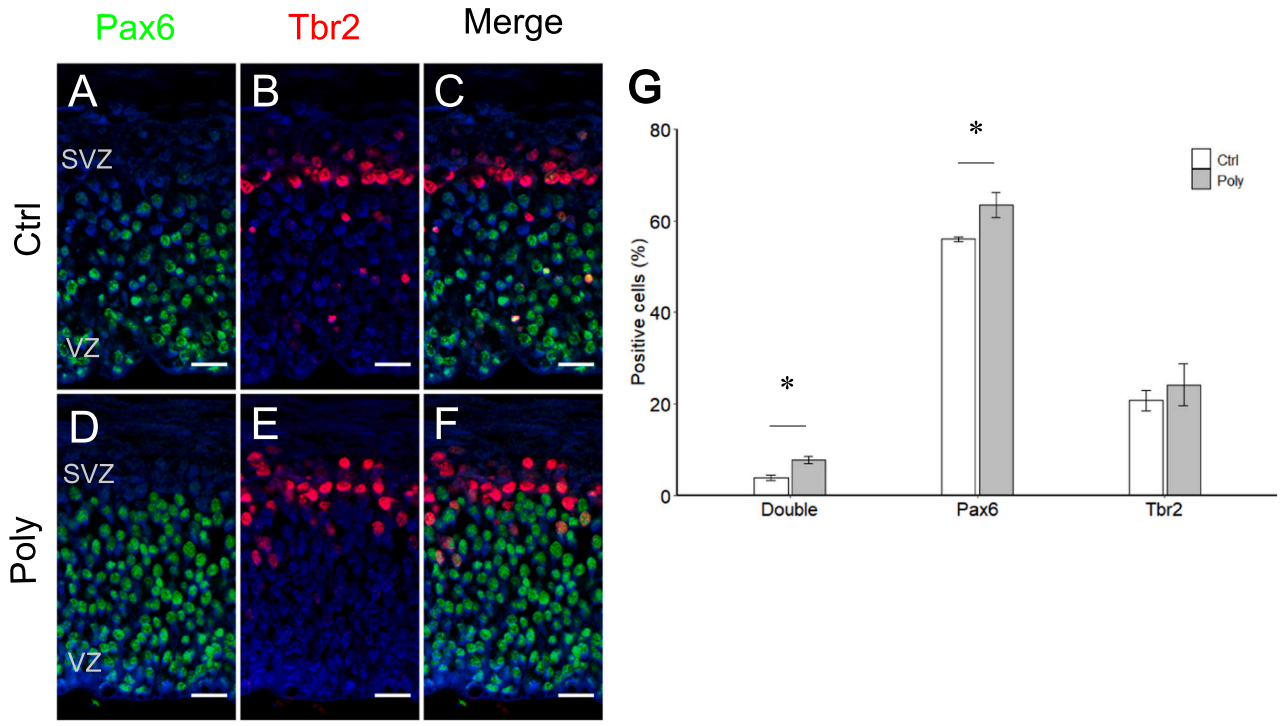

Fig. 1. Maternal immune activation leads to changes in the proportions of Pax6-positive progenitor cells at E13.5 (A-F) Representative immunofluorescence images of apical neural progenitor marker Pax6 and intermediate (or basal) progenitor marker Tbr2 on E13.5, 24 h after poly(I:C) injection. Scale bars, 20 μm in A-F. (G) The proportions of Pax6-positive progenitor cells (Ctrl: 55.9% ± 0.6%, Poly: 63.4% ± 2.3%), Tbr2-positive progenitor cells (Ctrl: 20.7% ± 2.5%, Poly: 24.2% ± 4.0%), and Pax6/Tbr2 double-positive progenitor cells (Ctrl: 3.8% ± 0.6%, Poly: 7.7% ± 0.6%) in the developing cerebral wall were quantified using the Qupath (v0.2.0) cell detection tool. For the saline group we used 3 dams and 6 fetuses, and for Poly(I:C): Poly, 4 dams, and 8 fetuses. ventricular zone: VZ, subventricular zone: SVZ. Data were analyzed using two-way ANOVA followed by Bonferroni post-tests. All values represent means ± SEM. *$p < 0.05$.

differentiation of NPCs (Englund et al., 2005). Therefore, there is a least possibility that both Pax6 and Tbr2 are increased in NPCs and that NPCs proliferate with being double positive state. Pax6 and Tbr2 double positive cells are defined as newly born BPs, considering the time course of marker expression of NPCs according to previous reports (Arai et al., 2011; Englund et al., 2005). There was no difference in the total number of cells per field in the developing cerebral wall (saline-injected group [n = 3]: 250.2 ± 10.3 cells, poly(I:C)-injected group [n = 4]: 225.1 ± 15.9 cells; values represent mean ± SEM). These findings suggested that MIA acutely increased the proportion of Pax6-positive cells and newly formed BPs.

MIA did not change the proportions of positive cells for Pax6, Tbr2, and Tbr1 at E 14.5

We next analyzed the composition of NPCs and the number of neurons at E14.5 with immunohistochemistry. In the saline-injected and poly(I:C)-injected groups, in addition to the location of Pax6-positive cells and Tbr2-positive cells in the VZ and SVZ, respectively, Tbr1-positive cells were located in the CP, as in normal brain development (Fig. 2A–H). Quantitative analysis showed there were no significant differences in the proportion of Pax6, Tbr2, and Tbr1-positive cells between the two groups (Fig. 2I). At E14.5, the proportion of newly formed BPs was not different between groups (Fig. 2I). In this analysis, regardless of the increased proportion of newly formed BPs at E13.5, we did not observe an increased proportion of postmitotic neurons 48 h after MIA (Fig. 2I). There was no difference in the total number of cells per field in the developing cerebral wall (saline-injected group: 416 ± 47.5 cells, poly(I:C)-injected group: 443.6 ± 27.4 cells, $n = 4$/group; values represent means ± SEM).

Both of apical and intermediate neural progenitor cells were increased in late pregnancy after MIA

To observe the number and distribution of NPCs in the late embryonic period after exposure to MIA at E12.5, we performed immunohistochemical analysis with two progenitor markers, Pax6 and Tbr2, at E18.5. Previously, we showed that Pax6-positive radial glial cells are decreased in wild-type mice between E11 and E18, and Tbr2-positive intermediate progenitor cells also decline between E13 and E18 (Radakovits et al., 2009). NPCs labeled with anti-Pax6 or -Tbr2 antibodies were relatively more abundant in the poly(I:C)-injected group (Fig. 3A–D). In cropped higher magnification images, Pax6 or Tbr2 positive cells were analyzed; Many Pax6- or Tbr2-positive cells were found in the SVZ in the poly(I:C)-injected group (Fig. 3E–I). In normal brain development, at this late stage, the proportion of these two types of progenitor cells decreased compared with that in the early stage, and these cells are localized only at the VZ (Englund et al., 2005). In the poly(I:C)-injected group, we could observe these cells in the SVZ, even in the late embryonic stage. These findings demonstrate that MIA may cause dysregulated corticogenesis.

GO enrichment analysis of DEGs in MIA-treated fetal brain showed cell response to various stress

We performed GO enrichment analyses using ShinyGO v0.61. Total

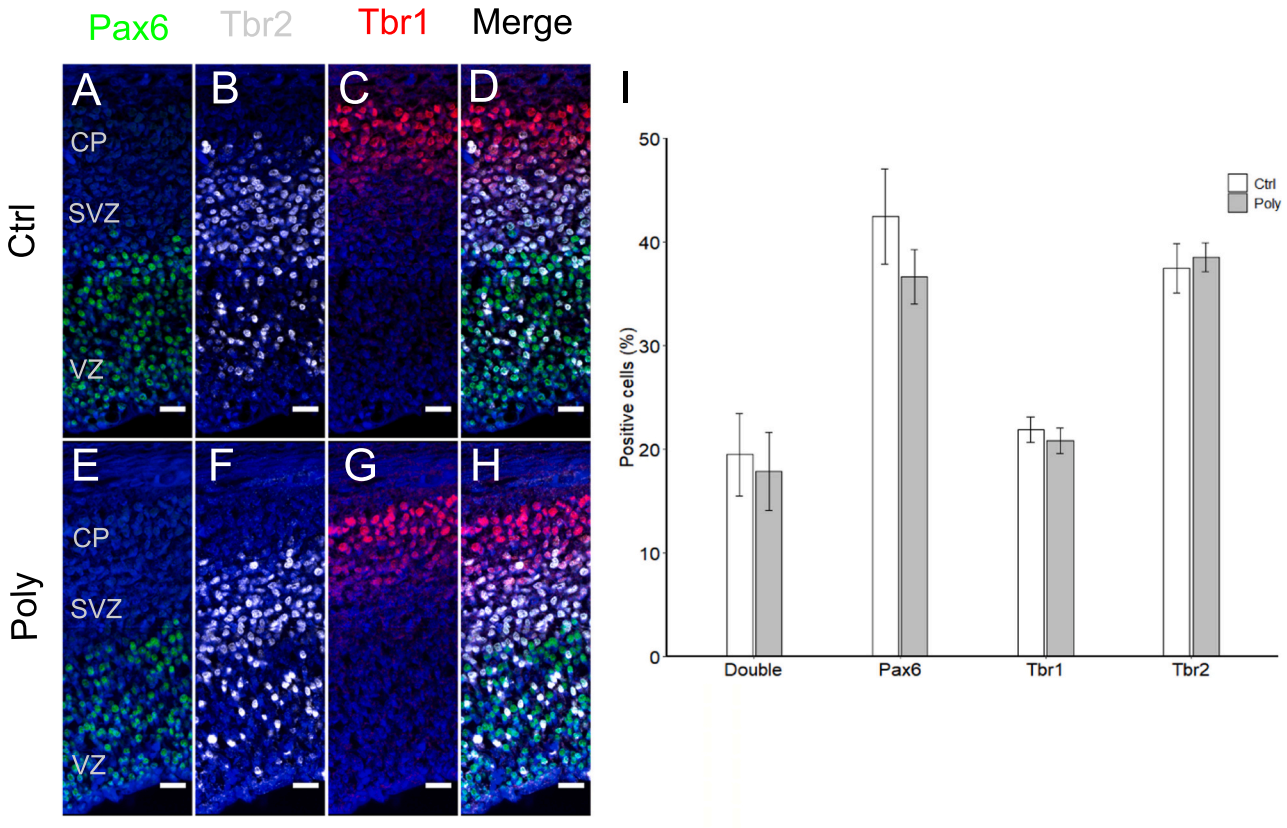

Fig. 2. Proportions of positive cells for Pax6, Tbr2, and Tbr1 at E 14.5 after MIA (A-H) Representative immunofluorescence images of Pax6, Tbr2, and Tbr1 on E14.5, 48 h after poly(I:C) injection (E14.5). Scale bars, 20 μm in A-H. (I) The proportions of Pax6-positive progenitor cells (Ctrl: 42.5 ± 4.0%, Poly: 36.6 ± 2.3%), Tbr2-positive progenitor cells (Ctrl: 37.4 ± 1.4%, Poly: 38.5 ± 0.6%), Tbr1-positive neurons (Ctrl: 21.9 ± 3.4%, Poly: 22.6 ± 3.3%), and Pax6/Tbr2 double-positive progenitor cells (Ctrl: 19.5 ± 2.0%, Poly: 16.4 ± 1.2%) in the developing cerebral wall were quantified using the QuPath (v0.2.0) cell detection tool. Control: Ctrl, Poly(I:C): Poly, $n = 4$/group, ventricular zone: VZ, subventricular zone: SVZ, cortical plate: CP. Data were analyzed by two-way ANOVA. All values represent means ± SEM.

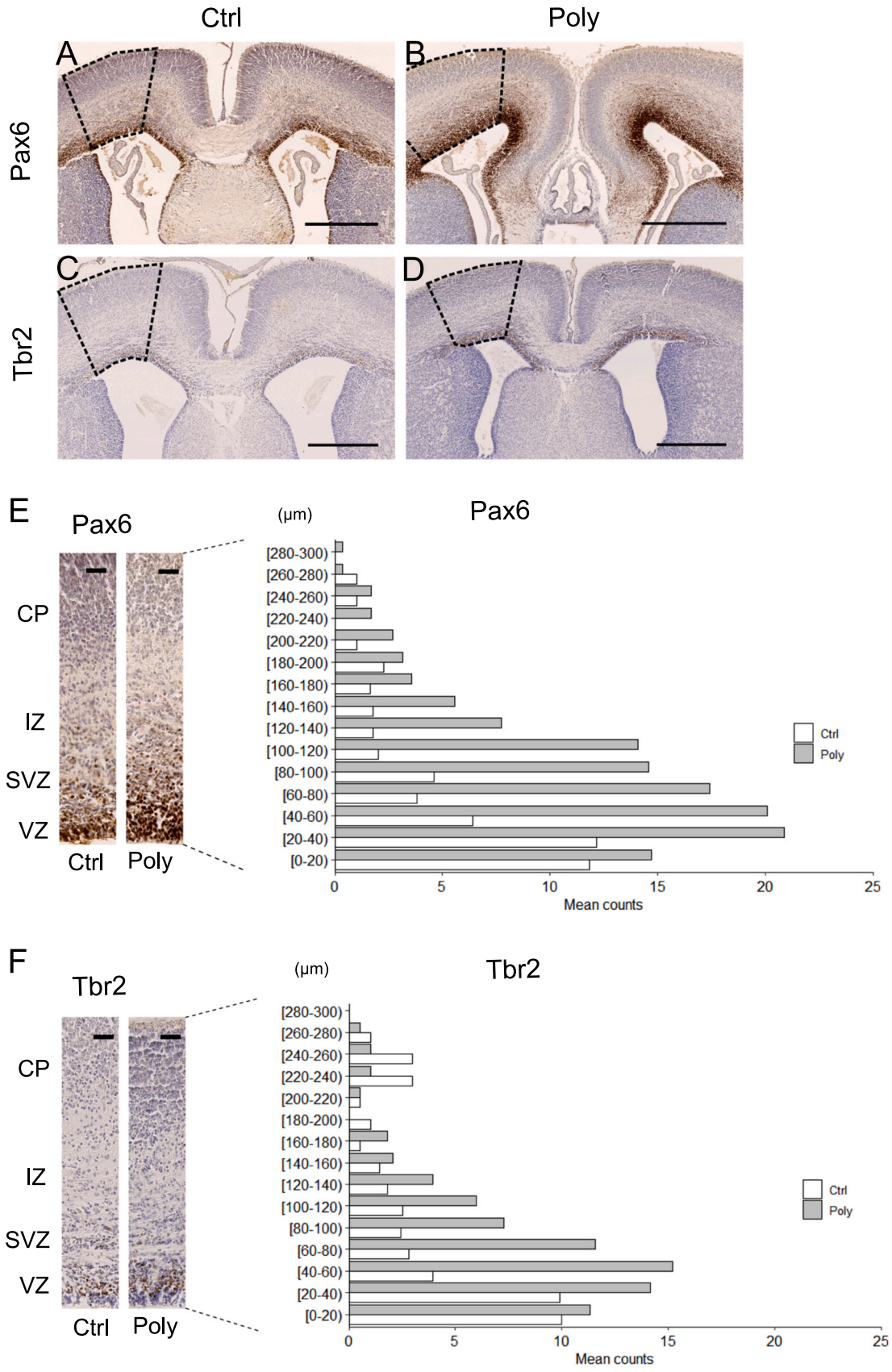

Fig. 3. Distribution of Pax6 and Tbr2 in fetal dorsal brain slices from saline-injected and poly(I:C) injected-mice on late gestation (E18.5). (A, B) Expression of Pax6 in the frontal region. (C, D) Expression of Tbr2 in the frontal region. (E) Distribution of Pax6-positive cells and mean cell numbers of each group at the width of 50 μm. (F) Distribution of Tbr2-positive cells and mean cell numbers of each group at the width of 50 μm. The dashed area in A-D depict the region of interest analyzed using Qupath software (v0.2.0). The bar graph shows the mean cell numbers in each group at the width of 50 μm. Control: Ctrl, Poly(I:C): Poly, ventricular zone: VZ, subventricular zone: SVZ, intermediate zone: IZ, cortical plate: CP, $n = 3$/group. Scale bars, 250 μm (A-D), 20 μm (E, H).

228 DEGs were extracted from published data (Garbett et al., 2012). Significantly over-represented GO terms of the DEGs are demonstrated in Fig. 4. In the top 40 significantly over-represented biological process terms, there were response to cytokine, response to decreased oxygen levels, innate immune response, and immune response. These responses are known to converge on the integrated stress response signaling pathway (Bueter et al., 2009; Lin et al., 2014; Pakos-Zebrucka et al., 2016). These results provide an insight into integrated stress response (ISR) and ER stress response in MIA-treated fetal brain.

MIA leads to upregulated Atf4 expression in the fetal brain

Following the previous GO enrichment analyses of DEGs induced by poly(I:C) injection, which showed the possibility of the involvement of integrated stress response, we examined the expression level of *Atf4*, which is known as an effector of integrated stress response. The level of Atf4 increased in the fetal brain in response to MIA at E13.5 (Fig. 5).

Discussion

In this study, we showed that MIA expands the pool of Pax6-positive NPCs and increases the process of indirect neurogenesis at 24 h; however, the number of postmitotic Tbr1-positive neurons in the developing cerebral wall was not different between the saline-injected group and the poly(I:C)-injected group at 48 h in a mouse model of maternal viral infection. Besides these results, we demonstrated that there were more Pax6-positive and Tbr2-positive NPCs in VZ/SVZ in the poly(I:C)-injected group than in the saline-injected group at E18.5. Specifically, Pax6-positive NPCs were located in SVZ as well as VZ. This means Pax6-positive NPCs were not in G1 cell cycle arrest. This is because apical NPCs are known for undergoing interkinetic nuclear migration (Salomoni and Calegari, 2010). In our previous study, we showed that MIA decreased S-phase NPCs labeled with 5-ethynyl-2-deoxyuridine after 48 h (Tsukada et al., 2015). These findings suggest that impaired neurogenesis is caused by a delay of cell cycle in NPCs. In another model of MIA, where maternal lipopolysaccharide (LPS) was injected, Stolp et al. showed that NPC proliferation decreased as early as within hours after MIA injection in mice (Stolp et al., 2011). They hypothesized that decreased NPC proliferation was induced by lengthening of the G1 phase, while still proceeding in the cell cycle and that more NPCs divided asymmetrically (Stolp et al., 2011). Despite the experimental differences between their study and ours, such as the maternal immune activator, timing of the injection, and time of histological analyses, the present results of increased Pax6-positive NPCs and Pax6/Tbr2 double-positive cells at E13.5 (24 h after MIA) would be compatible with the results of the LPS model. This is because we consider that cell cycle extension and impaired neuron production are fundamental events in MIA, regardless of maternal immune activator. As a potential

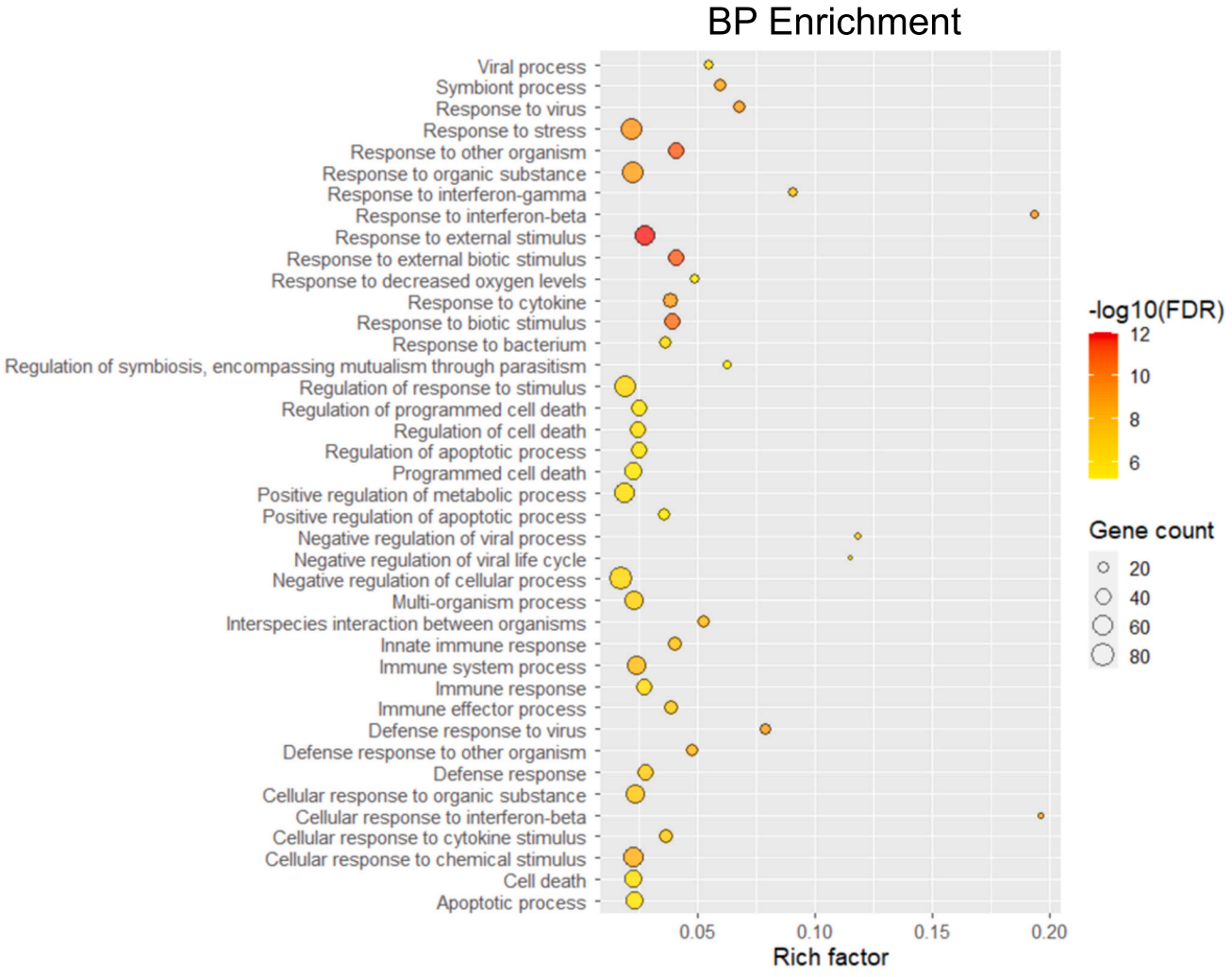

Fig. 4. GO enrichment analysis of DEGs in MIA-treated fetal brain. BPs in GO category. The x-axis shows the rich factor, which was calculated by the number of genes assigned to the GO term divided by the number of all genes in the background list. The order of the GO terms is alphabetical. The point size represents the count of genes enriched in a particular GO term. biological processes: BP.

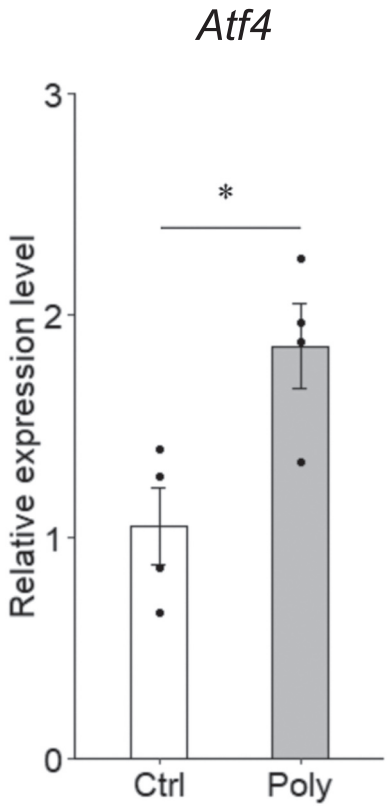

Fig. 5. Quantification of Atf4 expression in fetal brains exposed to MIA. mRNA levels of *Atf4* at E13.5. This was performed using samples from paraffin-embedded sections. Control: Ctrl, Poly(I:C): Poly, $n = 4$/group. All values represent means ± SEM. *$p < 0.05$.

underlying mechanism that could lead to impaired neurogenesis, we focused on the MIA-induced expression of Atf4 in the fetal brain because of the following reasons: 1) GO enrichment analyses of DEGs suggest that MIA acutely induced cell response to various stress in the fetal brain, including cytokines, decreased oxygen level, immune stimuli; In fact, it has been shown that hypoxia (Carpentier et al., 2013) and cytokine attack (Gallagher et al., 2013) had an effect on deregulated neurogenesis after MIA. These cells respond to hypoxia and cytokine converge on phosphorylation of the alpha subunit of eukaryotic translation initiation factor 2 (eIF2α), the core of ISR (Pakos-Zebrucka et al., 2016). 2) Atf4 is the main effector of ISR, which is caused by cytokines, hypoxia, and ER stress response (Bueter et al., 2009; Lin et al., 2014; Pakos-Zebrucka et al., 2016); and 3) Recent studies have shown that upregulation of Atf4-mediated UPR is correlated to microcephaly caused by direct prenatal Zika virus infection (Alfano et al., 2019; Gladwyn-Ng et al., 2018). Although we showed that Atf4 was upregulated in the fetal brain following MIA, indirect neurogenesis was not decreased in our results unlike in the direct Zika virus infection model and in a genetic model that induced Atf4-mediated UPR in developing mouse brains (Alfano et al., 2019; Laguesse et al., 2015). We consider that these discordant findings may arise from the severity of induced UPR, as previous work has shown that indirect neurogenesis other than neuron production was impaired in response to the stabilization of exogenous Atf4 in NPCs (Frank et al., 2010). As a potential mechanism by which Atf4 affects neurogenesis, it has been demonstrated that an overdose of Atf4 in NPCs can slow cell cycle progression and decrease neurogenesis (Frank et al., 2010). Based on these findings, we hypothesized that MIA impairs neurogenesis through upregulation of Atf4 in NPCs, leading to a delay of cell cycle exit. A latest published article has demonstrated that MIA induced ISR in the fetal brain at E14.5 and E18.5 and that blockade of ISR could rescue excessive neural activity and abnormal behaviors in the offsprings (Kalish et al., 2021), suggesting the causal relationship between ISR and MIA-induced phenotype. This notion suggests that ISR is also involved in the impairment of neurogenesis. One of limitations of our study is that we did not separately analyze the offsprings by sex. We examined UPR-related molecules, which are fundamental to maintaining cellular homeostasis, because recently Atf4-mediated UPR has been shown to regulate the balance of neurogenesis in the developing brain (Laguesse et al., 2015). However, evidence has indicated that environmental insults, such as MIA in the prenatal stage, have a higher affect in males. In future studies, sex must be examined as an experimental variable to understand the underlying mechanism by which MIA causes such phenotypes (Braun et al., 2019). In summary, our data showed that MIA impaired neurogenesis and upregulated Atf4 in the fetal brain. These findings will provide a new insight in the mechanism of MIA causing improper brain development and subsequent neurodevelopmental disorders.

Ethical statement

All procedures in this study were performed in strict accordance with the guidelines for the Care and Use of Laboratory Animals of Kanazawa Medical University, Ishikawa, Japan. The protocol was approved by the Committee on the Ethics of Animal Experiments of Kanazawa Medical University (Protocol number 2017-51).

CRediT authorship contribution statement

T.T, H.Shimada, H.S.-H, H.Shoji, and T.H conceived and designed the experiments. T.T conducted the experiments. T.T, H.S.-H, and T.H analyzed the data. T.T, H.Shimada, H.S.-H, H.Shoji, and T.H wrote the paper.

Conflicts of Interest

The authors declare no conflicts of interest.

Acknowledgments

Financial Support: This work was supported by JSPS KAKENHI (Grant Number 20K16938). The authors thank Tomoko Yasuda for her help with histological preparations. The authors would like to thank Enago (www.enago.com) for English language review.

References

Alfano, C., Gladwyn-Ng, I., Couderc, T., Lecuit, M., Nguyen, L., 2019. The unfolded protein response: a key player in Zika virus-associated congenital microcephaly. Front. Cell. Neurosci. 13, 94.

Arai, Y., Pulvers, J.N., Haffner, C., Schilling, B., Nüsslein, I., Calegari, F., Huttner, W.B., 2011. Neural stem and progenitor cells shorten S-phase on commitment to neuron production. Nat. Commun. 2, 154.

Atladóttir, H.O., Pedersen, M.G., Thorsen, P., Mortensen, P.B., Deleuran, B., Eaton, W.W., Parner, E.T., 2009. Association of family history of autoimmune diseases and autism spectrum disorders. Pediatrics 124, 687–694.

Bankhead, P., Loughrey, M.B., Fernández, J.A., Dombrowski, Y., McArt, D.G., Dunne, P. D., McQuaid, S., Gray, R.T., Murray, L.J., Coleman, H.G., James, J.A., Salto-Tellez, M., Hamilton, P.W., 2017. QuPath: open source software for digital pathology image analysis. Sci. Rep. 7, 16878.

Braun, A.E., Carpentier, P.A., Babineau, B.A., Narayan, A.R., Kielhold, M.L., Moon, H.M., Shankar, A., Su, J., Saravanapandian, V., Haditsch, U., Palmer, T.D., 2019. "Females Are Not Just 'Protected' Males": sex-specific vulnerabilities in placenta and brain after prenatal immune disruption. eNeuro 6.

Brown, A.S., Cohen, P., Harkavy-Friedman, J., Babulas, V., Malaspina, D., Gorman, J.M., Susser, E.S., 2001. Prenatal rubella, premorbid abnormalities, and adult schizophrenia. Biol. Psychiatry 49, 473–486.

Brown, A.S., Begg, M.D., Gravenstein, S., Schaefer, C.A., Wyatt, R.J., Bresnahan, M., Babulas, V.P., Susser, E.S., 2004. Serologic evidence of prenatal influenza in the etiology of schizophrenia. Arch. Gen. Psychiatry 61, 774–780.

Brown, A.S., 2006. Prenatal infection as a risk factor for schizophrenia. Schizophr. Bull. 32, 200–202.

Bueter, W., Dammann, O., Leviton, A., 2009. Endoplasmic reticulum stress, inflammation, and perinatal brain damage. Pediatr. Res. 66, 487–494.

Canetta, S., Bolkan, S., Padilla-Coreano, N., Song, L.J., Sahn, R., Harrison, N.L., Gordon, J.A., Brown, A., Kellendonk, C., 2016. Maternal immune activation leads to selective functional deficits in offspring parvalbumin interneurons. Mol. Psychiatry 21, 956–968.

Carpentier, P.A., Dingman, A.L., Palmer, T.D., 2011. Placental TNF-α signaling in illness-induced complications of pregnancy. Am. J. Pathol. 178, 2802–2810.

Carpentier, P.A., Haditsch, U., Braun, A.E., Cantu, A.V., Moon, H.M., Price, R.O., Anderson, M.P., Saravanapandian, V., Ismail, K., Rivera, M., Weimann, J.M., Palmer, T.D., 2013. Stereotypical alterations in cortical patterning are associated with maternal illness-induced placental dysfunction. J. Neurosci. 33, 16874–16888.

Choi, G.B., Yim, Y.S., Wong, H., Kim, S., Kim, H., Kim, S.V., Hoeffer, C.A., Littman, D.R., Huh, J.R., 2016. The maternal interleukin-17a pathway in mice promotes autism-like phenotypes in offspring. Science 351, 933–939.

Courchesne, E., Mouton, P.R., Calhoun, M.E., Semendeferi, K., Ahrens-Barbeau, C., Hallet, M.J., Barnes, C.C., Pierce, K., 2011. Neuron number and size in prefrontal cortex of children with autism. JAMA 306, 2001–2010.

Englund, C., Fink, A., Lau, C., Pham, D., Daza, R.A., Bulfone, A., Kowalczyk, T., Hevner, R.F., 2005. Pax6, Tbr2, and Tbr1 are expressed sequentially by radial glia, intermediate progenitor cells, and postmitotic neurons in developing neocortex. J. Neurosci. 25, 247–251.

Frank, C.L., Ge, X., Xie, Z., Zhou, Y., Tsai, L.H., 2010. Control of activating transcription factor 4 (ATF4) persistence by multisite phosphorylation impacts cell cycle progression and neurogenesis. J. Biol. Chem. 285, 33324–33337.

Gallagher, D., Norman, A.A., Woodard, C.L., Yang, G., Gauthier-Fisher, A., Fujitani, M., Miller, F.D., 2013. Transient maternal IL-6 mediates long-lasting changes in neural stem cell pools by deregulating an endogenous self-renewal pathway. Cell Stem Cell 13 (5), 564–576.

Garbett, K.A., Hsiao, E.Y., Kálmán, S., Patterson, P.H., Mirnics, K., 2012. Effects of maternal immune activation on gene expression patterns in the fetal brain. Transl. Psychiatry 2, 98.

Ge, S.X., Jung, D., Yao, R., 2020. ShinyGO: a graphical gene-set enrichment tool for animals and plants. Bioinformatics 36, 2628–2629.

Gilbert, J., Man, H.Y., 2017. Fundamental elements in autism: from neurogenesis and neurite growth to synaptic plasticity. Front. Cell. Neurosci. 11, 359.

Gladwyn-Ng, I., Cordón-Barris, L., Alfano, C., Creppe, C., Couderc, T., Morelli, G., Thelen, N., America, M., Bessières, B., Encha-Razavi, F., Bonnière, M., Suzuki, I.K., Flamand, M., Vanderhaeghen, P., Thiry, M., Lecuit, M., Nguyen, L., 2018. Stress-induced unfolded protein response contributes to Zika virus-associated microcephaly. Nat. Neurosci. 21, 63–71.

Godin, J.D., Creppe, C., Laguesse, S., Nguyen, L., 2016. Emerging roles for the unfolded protein response in the developing nervous system. Trends Neurosci. 39, 394–404.

Götz, M., Huttner, W.B., 2005. The cell biology of neurogenesis. Nat. Rev. Mol. Cell Biol. 6, 777–788.

Hong, S.J., Bernhardt, B.C., Gill, R.S., Bernasconi, N., Bernasconi, A., 2017. The spectrum of structural and functional network alterations in malformations of cortical development. Brain 140, 2133–2143.

Hsiao, E.Y., Patterson, P.H., 2011. Activation of the maternal immune system induces endocrine changes in the placenta via IL-6. Brain Behav. Immun. 25, 604–615.

Kalish, B.T., Kim, E., Finander, B., Duffy, E.E., Kim, H., Gilman, C.K., Yim, Y.S., Tong, L., Kaufman, R.J., Griffith, E.C., Choi, G.B., Greenberg, M.E., Huh, J.R., 2021. Maternal immune activation in mice disrupts proteostasis in the fetal brain. Nat. Neurosci. 24, 204–213.

Kreitz, S., Zambon, A., Ronovsky, M., Budinsky, L., Helbich, T.H., Sideromenos, S., Ivan, C., Konerth, L., Wank, I., Berger, A., Pollak, A., Hess, A., Pollak, D.D., 2020. Maternal immune activation during pregnancy impacts on brain structure and function in the adult offspring. Brain Behav. Immun. 83, 56–67.

Laguesse, S., Creppe, C., Nedialkova, D.D., Prévot, P.P., Borgs, L., Huysseune, S., Franco, B., Duysens, G., Krusy, N., Lee, G., Thelen, N., Thiry, M., Close, P., Chariot, A., Malgrange, B., Leidel, S.A., Godin, J.D., Nguyen, L., 2015. A dynamic unfolded protein response contributes to the control of cortical neurogenesis. Dev. Cell 35, 553–567.

Lin, M., Zhao, D., Hrabovsky, A., Pedrosa, E., Zheng, D., Lachman, H.M., 2014. Heat shock alters the expression of schizophrenia and autism candidate genes in an induced pluripotent stem cell model of the human telencephalon. PLoS One 9, 94968.

Livak, K.J., Schmittgen, T.D., 2001. Analysis of relative gene expression data using real-time quantitative PCR and the 2(-Delta Delta C(T)) method. Methods 25, 402–408.

Pakos-Zebrucka, K., Koryga, I., Mnich, K., Ljujic, M., Samali, A., Gorman, A.M., 2016. The integrated stress response. EMBO Rep. 17, 1374–1395.

Radakovits, R., Barros, C.S., Belvindrah, R., Patton, B., Müller, U., 2009. Regulation of radial glial survival by signals from the meninges. J. Neurosci. 29, 7694–7705.

Salomoni, P., Calegari, F., 2010. Cell cycle control of mammalian neural stem cells: putting a speed limit on G1. Trends Cell Biol. 20, 233–243.

Shi, L., Tu, N., Patterson, P.H., 2005. Maternal influenza infection is likely to alter fetal brain development indirectly: the virus is not detected in the fetus. Int. J. Dev. Neurosci. 23, 299–305.

Shin Yim, Y., Park, A., Berrios, J., Lafourcade, M., Pascual, L.M., Soares, N., Yeon Kim, J., Kim, S., Kim, H., Waisman, A., Littman, D.R., Wickersham, I.R., Harnett, M.T., Huh, J.R., Choi, G.B., 2017. Reversing behavioural abnormalities in mice exposed to maternal inflammation. Nature 549, 482–487.

Smith, S.E., Li, J., Garbett, K., Mirnics, K., Patterson, P.H., 2007. Maternal immune activation alters fetal brain development through interleukin-6. J. Neurosci. 27, 10695–10702.

Stolp, H.B., Turnquist, C., Dziegielewska, K.M., Saunders, N.R., Anthony, D.C., Molnár, Z., 2011. Reduced ventricular proliferation in the foetal cortex following maternal inflammation in the mouse. Brain 134 (Pt 11), 3236–3248.

Stoner, R., Chow, M.L., Boyle, M.P., Sunkin, S.M., Mouton, P.R., Roy, S., Wynshaw-Boris, A., Colamarino, S.A., Lein, E.S., Courchesne, E., 2014. Patches of disorganization in the neocortex of children with autism. N. Engl. J. Med. 370, 1209–1219.

Tsukada, T., Shimada, H., Sakata-Haga, H., Iizuka, H., Hatta, T., 2018. Molecular mechanisms underlying the models of neurodevelopmental disorders in maternal immune activation relevant to the placenta. Congenit. Anom.

Tsukada, T., Simamura, E., Shimada, H., Arai, T., Higashi, N., Akai, T., Iizuka, H., Hatta, T., 2015. The suppression of maternal-fetal leukemia inhibitory factor signal relay pathway by maternal immune activation impairs brain development in mice. PLoS One 10, 0129011.

Wegiel, J., Kuchna, I., Nowicki, K., Imaki, H., Wegiel, J., Marchi, E., Ma, S.Y., Chauhan, A., Chauhan, V., Bobrowicz, T.W., de Leon, M., Louis, L.A., Cohen, I.L., London, E., Brown, W.T., Wisniewski, T., 2010. The neuropathology of autism: defects of neurogenesis and neuronal migration, and dysplastic changes. Acta Neuropathol. 119, 755–770.

Wu, W.L., Hsiao, E.Y., Yan, Z., Mazmanian, S.K., Patterson, P.H., 2017. The placental interleukin-6 signaling controls fetal brain development and behavior. Brain Behav. Immun. 62, 11–23.